Cancer Imaging

The current status and future prospects for molecular imaging-guided precision surgery

Imke Boekestijn[1,2], Matthias N. van Oosterom[1], Paolo Dell'Oglio[1,3], Floris H. P. van Velden[4], Martin Pool[5], Tobias Maurer[6], Daphne D. D. Rietbergen[1,2], Tessa Buckle[1] and Fijs W. B. van Leeuwen[1*]

Abstract

Molecular imaging technologies are increasingly used to diagnose, monitor, and guide treatment of i.e., cancer. In this review, the current status and future prospects of the use of molecular imaging as an instrument to help realize precision surgery is addressed with focus on the main components that form the conceptual basis of intraoperative molecular imaging. Paramount for successful interventions is the relevance and accessibility of surgical targets. In addition, selection of the correct combination of imaging agents and modalities is critical to visualize both microscopic and bulk disease sites with high affinity and specificity. In this context developments within engineering/imaging physics continue to drive the growth of image-guided surgery. Particularly important herein is enhancement of sensitivity through improved contrast and spatial resolution, features that are critical if sites of cancer involvement are not to be overlooked during surgery. By facilitating the connection between surgical planning and surgical execution, digital surgery technologies such as computer-aided visualization nicely complement these technologies. The complexity of image guidance, combined with the plurality of technologies that are becoming available, also drives the need for evaluation mechanisms that can objectively score the impact that technologies exert on the performance of healthcare professionals and outcome improvement for patients.

Keywords: Image-guided therapy, Intraoperative molecular imaging, Surgery, Fluorescence imaging, Multimodal imaging, Digital surgery, Surgical navigation, Pharmacokinetics

Introduction

Molecular imaging is increasingly being used to diagnose a range of diseases and to monitor and guide therapy, particularly in cancer. In this setting, molecular imaging often aids in the selection of systemic versus locoregional therapies [1]. The combination of diagnostics and therapy is commonly referred to as theranostics. In the nuclear medicine imaging literature, this approach typically refers to the application of radionuclide therapy based on demonstration of high expression of a therapeutic target presented on a diagnostic scan using PET or SPECT.

However, a less-well recognized aspect of theranostics is the use of imaging to guide device-based interventions. Prime examples include percutaneous needle placement [2] and liver embolization [3]. These approaches are generally guided by imaging techniques such as ultrasound, or CT and SPECT 'scout' scans. Image-guided therapy equally applies to surgery, a field where precision planning can directly impact patient care. Image guidance can in particular be used to illuminate surgical targets (diseased tissue) or non-targets (healthy tissue that needs to be spared).

In surgery, favorable outcomes are achieved by excising all diseased tissue. At the same time the severity of complications is related to the invasiveness of an intervention. Hence, a balance needs to be created between the need for radical removal of disease and

*Correspondence: f.w.b.van_leeuwen@lumc.nl

[1] Interventional Molecular Imaging Laboratory, Department of Radiology, Leiden University Medical Center, Leiden, the Netherlands
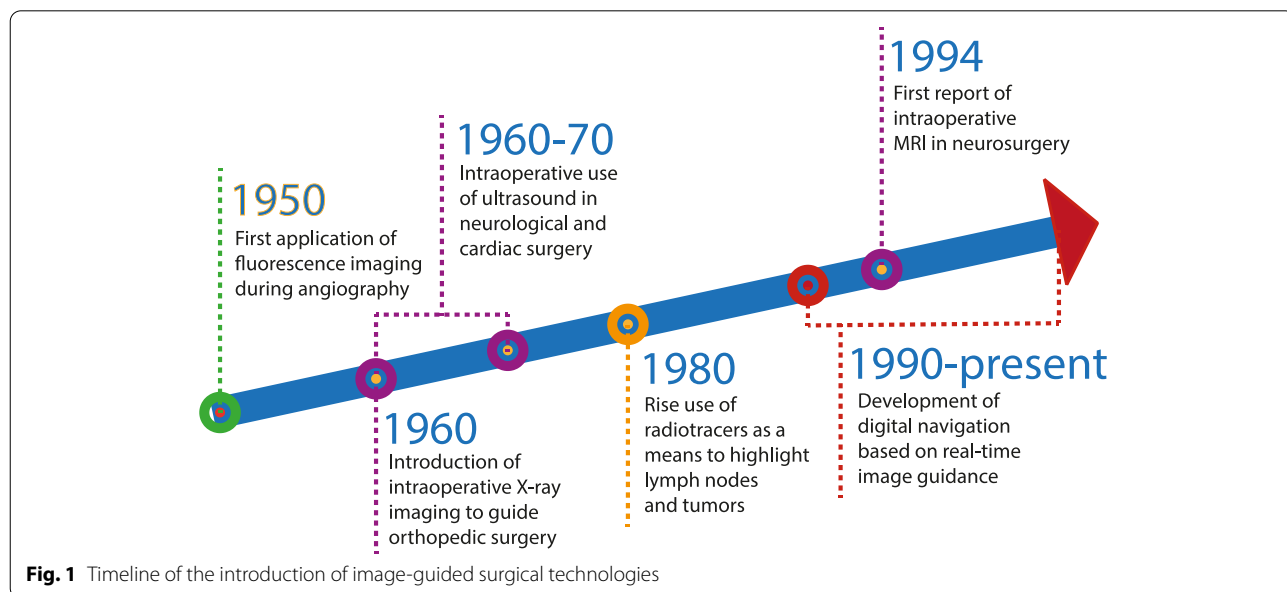Full list of author information is available at the end of the article

Boekestijn *et al. Cancer Imaging*   (2022) 22:48

Page 2 of 15

minimizing the scope of surgery. Accordingly, there is a drive towards minimal-invasive and more personalized interventions, while providing patients and healthcare professionals more confidence in the efficacy of radical resection, as well as uncomplicated postoperative recovery. From the very beginning of surgical practice decision-making has been guided by the tactile and visual senses of the operating surgeon. The technological advances made in the last century now allow these senses to be complemented via the use of preoperative imaging roadmaps (e.g., CT, MRI, SPECT and PET) and intraoperative target visualization in the form of white-light endoscopic video-image guidance. This evolution is helping minimally invasive 'key-hole' approaches to gradually replace open surgery. A clear example is the rise of robot-assisted laparoscopic surgery [4], which some now consider the standard-of-care in the resection of prostate cancer [5, 6]. The flip side of this minimally invasive trend is the loss of "touch" and thus a growing reliance on image guidance. An obvious next step in advancing image guidance in minimally invasive surgery is the inclusion of intraoperative molecular imaging strategies. Such strategies can help assist in target identification to guide resection of disease sites more accurately, while preserving delicate healthy anatomy and have led to the development of the concept of image-guided surgery [7, 8].

Historically, image-guided surgery has been pursued using different modalities. Since the late 1950s fluorescence imaging has been implemented during angiography ([9–11]; Fig. 1). In the 1960s, intraoperative X-ray devices started to be used to provide imaging as guidance for orthopedic surgical interventions [12] and intraoperative ultrasound (US) was introduced to guide surgeons during neurological and cardiac surgery. The latter became more widely accepted in the late 1970s, mainly for application in general surgery [13]. Since the 1980s, radioactive tracers (radiotracers) have been implemented to highlight lymph nodes [14, 15], and later tumors [16]. Although scarce, there have even been reports describing the use of intraoperative magnetic resonance imaging during neurosurgery (first report in 1994, [17]). More exotic modalities are the use of magnetic particles [18, 19], optoacoustics [20], and Raman spectroscopy [21]. Digital navigation based on preoperative computed tomography (CT) or magnetic resonance imaging (MRI) roadmaps has been seen since the 1990's with examples in head-and-neck, neuro- and orthopedic surgery [22]. Combined these approaches provide the foundations for evolving image-guided surgery.

The success of image-guided surgery is driven by the synergy between four main generic components: 1) relevance and accessibility of the target (medicine), 2) imaging agents (chemistry/pharmacology/pharmaceutics), 3) modalities used to detect or navigate towards the target defined in via imaging (engineering/imaging physics), and 4) interpretation of the imaging data (computer visualization). In this review, the status and future prospects of these four aspects of image-guided surgery is addressed. In addition, we indicate how each of the components can contribute to transition of new concepts from a laboratory setting into standard clinical care pathways (translational medicine).

Fig. 1 Timeline of the introduction of image-guided surgical technologies

Boekestijn *et al. Cancer Imaging*   (2022) 22:48

Page 3 of 15

Results

Target tissues

The concept of image-guided surgery has been most extensively pursued in the field of oncology. In this setting, molecular imaging has helped raise the diagnostic standard and increase the accuracy with which target tissues can be non-invasively identified. Key aspects herein are exemplified by the synergies of modalities such as positron emission tomography/computed tomography (PET/CT) with receptor-specific radiotracers such as [^{68} Ga]-octreotate, [^{68} Ga]-DOTATOC [23] and [^{68} Ga]-PSMA-11 [24]. Through this combination nuclear medicine has been able to demonstrate that receptor-mediated imaging based on tumor cell-related receptor overexpression allows accurate patient staging of lesions that are > 2 mm in diameter. Thereby enabling the identification of patients who may be suitable for surgical resection with curative intent.

Image guidance is routinely used to clearly delineated organs such as blood vessels (angiography; indocyanine green (ICG; [25], US [26], X-ray [27]), bile ducts (ICG [28]), parathyroid (autofluorescence [29, 30]), lymph nodes (ICG and fluorescein [31, 32]), bony structures (X-ray; [33]), and macroscopic tumor lesions (US, 5-ALA; [34, 35], Fig. 2). Despite the widespread implementation of these applications the real promise of image guidance lies perhaps in indications wherein radical resection of microscopic or diffuse infiltrative lesions is required, with adequate safety margins. Unfortunately, application of image guidance in these indications also provides the toughest challenges as it requires a combination of tracers with high affinity and specificity for diseased tissue, and the generation of target to background cont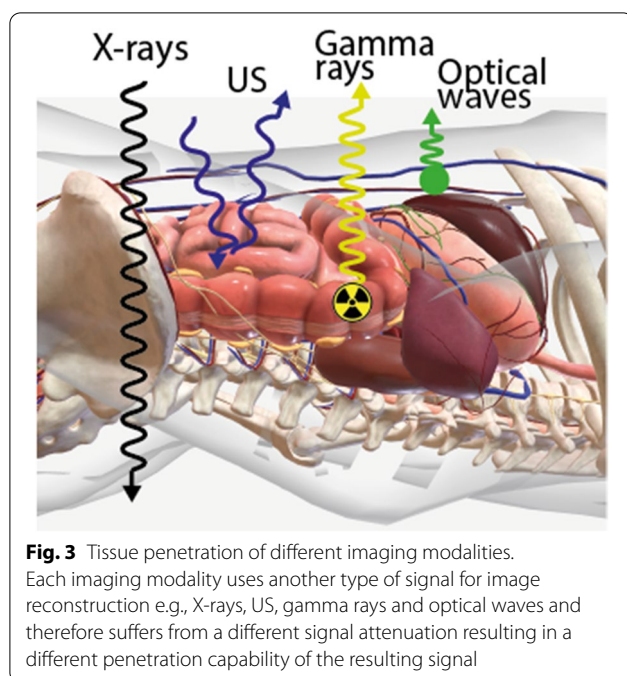rast that allows accurate detection with the chosen instrumentation. An important drawback herein is that diffuse infiltrative cancers may directly translate into low signal intensities, limiting sensitivity for image guidance. The effect of signal intensity becomes even more important when realizing that during excision a safety margin in the range of 5–10 mm often has to be applied. This means that detection needs to be efficient through a substantial amount of tissue and therefore attenuation and scattering of signal are important considerations.

From the perspective of having high signal intensity and low background, radiotracers are generally superior to optical tracers (including optoacoustics and lifetime imaging). With regard to having low signal attenuation and being subject to scattering, X-ray is the superior modality, followed by radiotracer-based detection, then US and lastly, optical tracers ([36, 37], Fig. 3). An important limitation for all optical approaches is that these are subjected to tissue-interactions during target illumination and/or signal emission; an effect that is smallest for optoacoustic applications [38]. Next to the issue of sensitivity, identification of small lesions requires an imaging modality with a high spatial resolution. Herein optical technologies, and in particular fluorescence, are superior compared to respectively US, radiotracer-based and X-ray detection.

When looking at the practical implementation of the above-mentioned modalities, some basic principles can be deduced. First and foremost, all routine optical imaging indications remain confined to superficial assessment (e.g., endoscopic procedures of the mucosal surface of the bowel or airways), whereby the impact of light attenuation of the emitted signal and background light can be kept to a minimum. In addition, these applications tent to rely on relatively 'simple' chemicals. In a relatively high
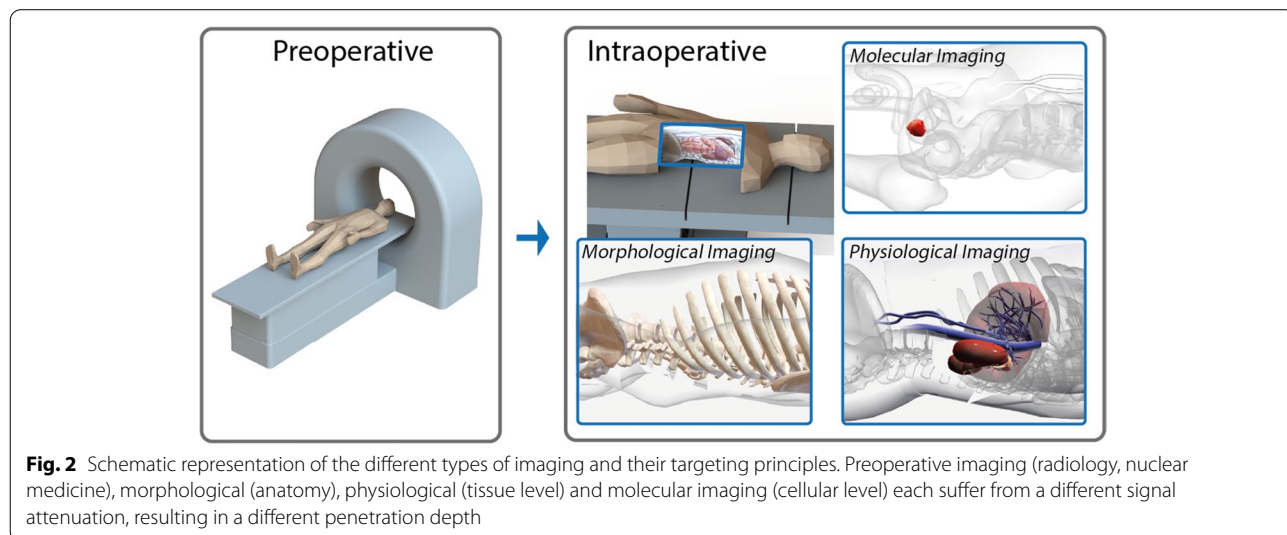
Fig. 2 Schematic representation of the different types of imaging and their targeting principles. Preoperative imaging (radiology, nuclear medicine), morphological (anatomy), physiological (tissue level) and molecular imaging (cellular level) each suffer from a different signal attenuation, resulting in a different penetration depth

Boekestijn *et al. Cancer Imaging*   (2022) 22:48

Page 4 of 15

Fig. 3 Tissue penetration of different imaging modalities. Each imaging modality uses another type of signal for image reconstruction e.g., X-rays, US, gamma rays and optical waves and therefore suffers from a different signal attenuation resulting in a different penetration capability of the resulting signal

dose these agents help study physiological aspects such as vascular-, lymphatic-, and bile- flow [39]. Compared to optical imaging, US can help to increase the detection depth up to a certain degree and allows for real-time dynamic visualization. That said, this modality does not really facilitate molecular imaging beyond the targeting of receptors in the epithelium of blood vessels due to the lack of contrast extravasation. Optoacoustics, on the other hand, provides an interesting integration of the favorable optical high spatial resolution and US characteristics. However, for lesions located deeper below the tissue surface detection based on radioactive signals is preferred. This preference is not only driven by the modality's signature to be able to penetrate overlaying tissue during the resection, but is also strengthened by the ability to non-invasively create a preoperative 'imaging roadmap' that accurately visualizes the distribution of the imaging agent (preferably in three-dimensions (3D, [40–42]). Such a roadmap allows the operating surgeon to only pursue a targeted resection when there is sufficient evidence that lesions are effectively identified. In addition, this preoperative roadmap helps to accurately locate (satellite) lesions that lie beyond traditional dissection templates [43]. While intraoperative CT [44] or MRI [45] also facilitate surgical planning via similar 3D roadmaps, the low contrast sensitivity of these modalities makes them less suitable for molecular imaging [46]. Hybrid approaches wherein the strengths of individual modalities are integrated could realise a best-of-both-worlds scenario [47, 48].

Trends in imaging agents for surgery

The range of applications wherein interventional molecular imaging is having clinical impact is increasing through advances in medical chemistry and radiochemistry. In particular, there has been significant development in the design of optical- (e.g., fluorescence, Cherenkov, optoacoustics, Raman) and radioisotope-based (e.g., gamma rays and beta particles) agents [49, 50].

From a chemical perspective, most of the efforts towards designing disease specific imaging agents find their origins in nuclear medicine and its subdiscipline of radiochemistry. Radioguided surgery applications for sentinel nodes (radiocolloids, [51]), somatostatin receptor overexpressing lesions (peptides, [52, 53]) and prostate specific membrane antigen (PSMA) expressing lesions (small molecules, [54]) have established ^{99m}Tc (140 keV) and, to a lesser extent, ^{111}In (gamma rays with photon energies of 171 and 245 keV) as the most favorable radioisotopes [55] for clinical use. This is primarily driven by the common availability of ^{99}Mo/^{99m}Tc generators in clinics world-wide and ^{111}In being an accessible long-lived reactor product. This further focused tracer design, with recent examples of widely implemented agents being ^{99m}Tc-PSMA-I&S [56], (ICG-)^{99m}Tc-nanocolloid [48] and ^{111}In-octreotide [57]. Besides the application-specific design of radiotracers there are various attempts to use off-the-shelve PET tracers for image guidance by exploring i.e., their 511 keV gamma rays [58], beta particles [59] and/or Cherenkov light [60]. Advantages of the use of radiotracers are that they can be applied under a micro-dosing regime, are compatible with quantitative biodistribution studies (%ID/g) and support non-invasive pre-operative imaging approaches such as scintigraphy, single photon emission computed tomography (SPECT) and PET (Table 1).

Second in popularity is the development of fluorescent tracers intended for superficial lesion identification. Where fluorescence microscopy tends to focus on use of dyes in the 400-700 nm range, fluorescence-guided surgery efforts often tend to explore the theoretically favorable interaction between near-infrared (NIR) fluorescence (>750 nm) and tissue [117]. NIR wavelengths are said to allow deeper penetration depth without visual obstruction of the surgical field caused by the dye. Interestingly, there is mounting evidence that fluorescence emissions outside of the NIR range equally hold promise for in-human use [118], with a prime example being the FDA-approved use of 5-ALA in neurosurgery [79]. While fluorescence imaging cannot be used to obtain preinterventional roadmaps, fluorescent agents are increasingly used in combination with some form of diagnostic nuclear medicine scan (see Table 1 for examples). This concept is most valid when the fluorescent and nuclear

Table 1 Examples of radio-, fluorescent and hybrid tracers used for preoperative imaging and intraoperative guidance

	Preoperative imaging	Intraoperative guidance	Hybrid tracer
Blood flow	Gd-DTPA (MRI; [61]), Iomeron (CT; [62]), Optison (US; [63])	ICG (fluorescence; [64]), Fluorescein (fluorescence; [65])	-
Sentinel lymph nodes	Radiocolloids * (SPECT; [66])	Radiocolloids * (γ probe; [66]), SPIONs (magnetic probe; [67]), ICG (fluorescence; [66]), Fluorescein (fluorescence; [68])	ICG-^{99m}Tc-nanocolloid (γ probe and fluorescence; [66])
Biliary excretion	^{99m}Tc-mebrofenin (SPECT; [69]), ^{99m}Tc-disofenin (SPECT; [70])	ICG (fluorescence; [71])	-
(Para)thyroid	$^{123/131}$I-pertechnate (SPECT; [72]), ^{99m}Tc-sestamibi (SPECT;[73]), Iodine (SPECT; [74])	ICG (fluorescence; [75]), $^{123/131}$I-pertechnetate (γ probe; [76]), ^{99m}Tc-sestamibi (γ probe; [77]), autofluorescence (fluorescence), Iodine (γ probe; [77])	^{124}I (Beta-probe, Cerenkov imaging; [55]), ^{123}I-Methylene Blue (γ probe visual blue; [77])
Metabolism	^{18}F-FDG (PET; [55]), $^{123/131}$I-MIBG (SPECT; [78])	5-ALA (PpIX; fluorescence; [79–81]), ^{125}I-MIBG (γ probe; [82])	-
Receptor targeted			
Prostate cancer (PSMA)	^{68}Ga-PSMA (PET; [83]), ^{18}F-PSMA (PET; [84]), ^{99m}Tc-PSMA-I&S (SPECT; [40])	^{68}Ga-PSMA (beta-probe; [83]), ^{99m}Tc-PSMA I&S (γ probe; [40])	^{68}Ga-PSMA (beta-probe and Cerenkov; [85]), ^{68}Ga-Glu-urea-Lys-(HE)$_3$-HBED-CC-IRDye800CW (PET and fluorescence; [86])
Somatostatin	^{68}Ga-DOTATOC (PET; [87, 88]), ^{111}In-octreotide (SPECT; [89]), ^{99m}Tc-depreotide (SPECT; [90]), ^{68}Ga-DOTATATE (PET; [91])	^{68}Ga-DOTATOC (beta probe; [55]), ^{111}In-octreotide (γ probe; [53]), ^{99m}Tc-depreotide (γ probe; [53])	-
Tyrosine-protein kinase Met (C-Met)	^{68}Ga-EMP-100 (PET; [92])	EMI-137 (fluorescence; [93, 94])	-
Integrins (α$_v$b$_3$)	^{68}Ga-RGD (PET; [95]), ^{18}F-RGD (PET; [96])	cRGD-ZW800-1 (fluorescence; [97])	^{124}I-cRGDY-PEG-C (beta probe, fluorescence; [98])
Vascular endothelial growth factor (VEGF)	^{89}Zr-Bevacizumab (PET; [99])	CW800-Bevacizumab (fluorescence; [100]),	-
Human epidermal growth factor-2 (Her-2)	^{68}Ga-Her2 (PET; [101])	CW800-HER2 (fluorescence; [102])	^{111}In-HER2-IRDye800CW (γ probe, fluorescence; [103])
Carcinoembryonic Antigen (CEA)	^{111}In-DTPA (SPECT; [104]), ^{111}In-IMP288 (SPECT; [105])	FITC-CEA mAb (fluorescence; [106]), SGM-101 (fluorescence; [107])	^{111}In-DTPA-SGM-101) (γ probe, fluorescence; [104]), FITC-^{125}I- CEA mAb (γ probe, fluorescence; [108])
Epidermal growth factor receptor (EGFR)	^{89}Zr-Cetuximab (PET; [109])	cetuximab-IRDye800 (fluorescence; [110–112]), panitumumab-IRDye800 (fluorescence; [113])	-
Carbonic Anhydrase IX	^{89}Zr-Girentuximab (PET; [114]), ^{124}I-redectane (PET; [115])	-	^{111}In-DOTA- Girentuximab-IRDye800CW (γ probe, fluorescence;[116])

* e.g. ^{99m}Tc-(nanocolloid, Senti-Scint, phytate colloid, tin colloid, sulfur colloid)

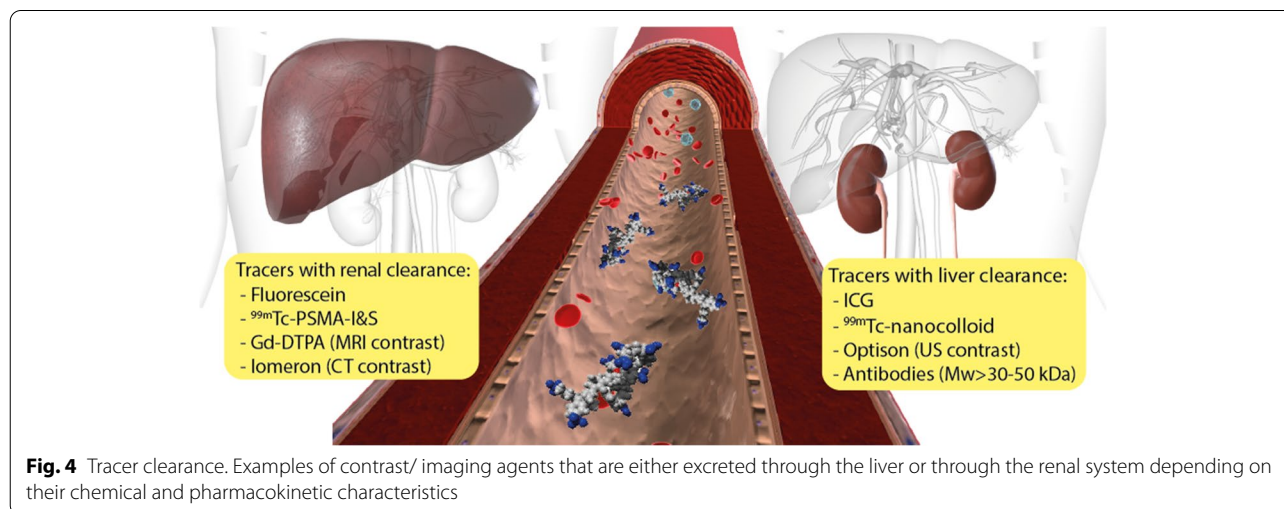Boekestijn *et al. Cancer Imaging*   (2022) 22:48

Page 6 of 15

agents have the same target affinity, pharmacokinetics and can be applied in the same dosing regimen. Unfortunately, the molecular properties of the relatively 'bulky' fluorescent labels can exert a substantial influence on the affinity and pharmacokinetics of small-molecule and peptide-based tracers [119]. There is even literature suggesting that fluorescent dyes may alter the pharmacokinetics of 'large' nanobodies [120] and antibodies [121]. An additional downside of fluorescent agents is that their biodistribution cannot be assessed quantitatively based on fluorescence intensity alone, due to autofluorescence, signal scattering and limited tissue penetration of the signal. Moreover, in contradiction to the low administered mass of radiotracers and subsequent lack of biological effects with most agents [122], fluorescent tracers tend to be used at pharmacologically-active dose levels [123]. Use of such high dose levels may reduce the number of false negative results but is also likely to increase non-specific (background) staining. This enhances the number of both false negatives (due to loss of contrast) and false positive results. Hereby is it must be noted that fluorescent dye properties such as lipophilicity, charges and level of serum binding influence the pharmacokinetics, in particular the mechanism of clearance (Fig. 4). For obvious reasons the effect of the latter can be quite critical when the surgical target is located directly within (e.g., kidney or liver) or immediately downstream of the renal of hepatobiliary clearance route (e.g., prostate or bowel) where unbound excreted tracer can severely hamper lesion identification.

A strategy to overcome the limitations of individual modalities is the use of bimodal/hybrid imaging agents. Herein, nuclear medicine signals tend to be complemented with optical [124], magnetic [125], or US [126] contrast. In particular, nuclear/optical applications have demonstrated value in the surgical setting [50]. Combining two signatures in a single imaging agent allows for detection by two independent modalities, thereby supporting all relevant aspects in pre- and intraoperative imaging. As can be derived from the above, such hybrid agents will have different detection sensitivities for the different signatures. Ideally, the fluorescence sensitivity of hybrid agents is improved. However, the means to do so are limited. Hereby it is important to note that self-quenching of fluorescent dyes occur when dyes that reside on the same molecule are located within 8 nm of each other [127, 128]. For most imaging agents this means that there is an optimum in the number of dyes used as label e.g., 1 to 1 molar ratio [129]. This essentially means that improvements can only be realized by tuning the fluorescence brightness of dyes (a multiplication between i.e., molar extinction coefficient and the quantum yield). The most common dyes used in image-guided surgery applications are cyanine dyes, wherein extension of the length of the $-C=C-$ bridge facilitates the use of higher wavelengths, but at the same yields suboptimal trans-confirmations [130]. As a result analogues of the cyanine dye Cy7.5 such as the commonly used ICG have a low brightness [131]. Introduction of charged moieties e.g. $-SO_3^-$ has been shown to enhance the brightness [132].

Trends in medical devices for interventional imaging

The ideal intraoperative detection modality would probably be best described as a device that: 1) has a high sensitivity for signal detection, 2) only marginally suffers from interference by non-specific background signal (high specificity) and 3) maintains or improves present surgical logistics. These are generic wishes that transcend across all modalities.

Fig. 4 Tracer clearance. Examples of contrast/ imaging agents that are either excreted through the liver or through the renal system depending on their chemical and pharmacokinetic characteristics

It is no surprise that the imaging physics drive the design of a medical device used for interventional imaging. Conventional X-ray approaches such as CT and fluoroscopy are often impractical for implementation in the surgical suite, and accordingly, surgical interventions more often implement X-ray imaging in the form of a c-arm design [133]. In some cases, even C-arms prove to be incompatible with the surgical setup [134]. US requires a relatively small transducer that contains an integrated pulsed sound source and detector capable of registering reflected sound waves [135]. As air interferes with the detection, the transducer needs to be placed in direct contact to tissue, often requiring the use of conductive gel. Optical technologies such as fluorescence imaging does not require direct contact with tissue for a light source to excite fluorophore molecules and a detector to collect the light that is subsequently emitted [136]. Since light sources including ambient light [137], plenum light [138] and light emitted by optical tracking systems [139] can interfere with signal detection, fluorescence applications often require dimming of interfering light sources such as the operating room (OR) lights. Radioguidance modalities are purely designed to detect radiopharmaceuticals that intrinsically generate a signal (i.e., gamma rays or beta particles). However, to determine the position of the emission source within the patient (i.e., the radiopharmaceutical), collimation is required. Interestingly, surgical modalities have also been combined in hybrid, or multimodal, devices. Examples being: a C-arm with integrated gamma detector [140], gamma detector with integrated fluorescence imaging [141], several versions of SPECT or gamma detection integrated with US [142, 143] and beta detection integrated with optical coherence tomography [144].

Effective application of imaging modalities during surgery is highly dependent on the degrees of freedom with which the modality can be positioned relative to the target. In open surgery (Fig. 5), cameras are not necessarily restricted in size other than the footprint that they occupy in the OR and the investment costs. Handheld probes (gamma [145], fluorescence [146], US, and magnetic [147]) as well as mobile gamma and fluorescence cameras [148] set the standard today (Fig. 5). The designs of these modalities can vary substantially. For example, probes are often provided in different detection angles (e.g., 0°, 45° and 90°) and mobile cameras are available as handheld device (e.g., Crystal cam [149], PDE-neo II [148]) or attached to a mechanical positioning arm (e.g., Sentinella or VITOM). Detection angles and size reductions can facilitate the accessibility of certain restricted anatomies, while mechanical arms offer stable positioning but often result in loss of dynamic flexibility. Taking fluorescence-guided surgery systems as an example, enlargement of detectors and excitation light sources can provide a boost in sensitivity [148]. This is a feature that may substantially increase utility, but also comes with increases in cost. While common practice, improvements in sensitivity do not necessarily result in an
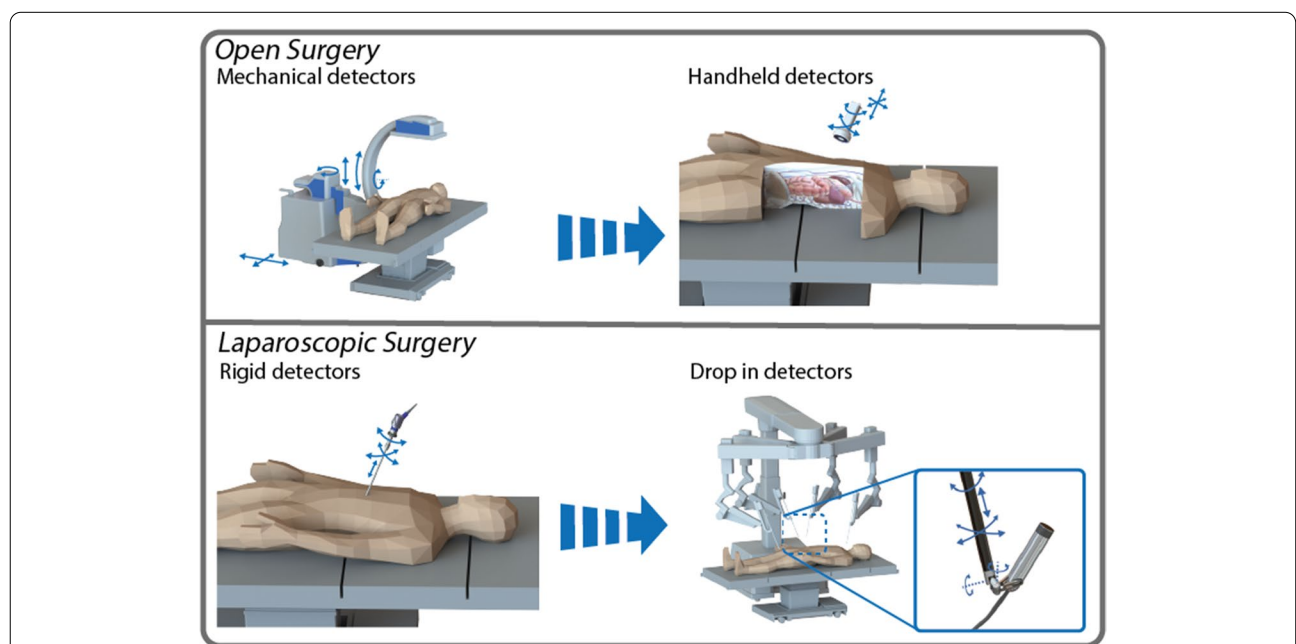
Fig. 5 Detectors in open and laparoscopic surgery. The various kind of intraoperative detectors used for image guided surgery (open and laparoscopic) including their movement's degrees of freedom

Boekestijn *et al. Cancer Imaging*   (2022) 22:48

Page 8 of 15

enlarged footprint, as they may also come from improved detector materials and refined signal processing [106, 138].

A stated earlier surgery is increasingly performed in a minimally invasive setting (Fig. 5, laparoscopic surgery). While the signals that need to be detected tend to stay the same, this change in environment requires a substantial change in the design of an imaging modality. The main driving factor herein can be attributed to the physical restrictions that are inherent in "key-hole surgery", meaning that the entry point limits both instrument size and movements [150, 151]. Interestingly, minimally invasive interventions tend to go hand-in-hand with the loss of tactile sensing and thus, increasing the demand for 'molecular-sensing' technologies. For such modalities miniaturization is the focus of the current general design trend. In most instances this translates to a loss in sensitivity when compared to the open surgery setting. A key example herein is fluorescence guidance [152]. Uniquely for radioguided surgery the gamma-detectors used in probes remain similar for both the open and laparoscopic devices, thus preserving sensitivity [150]. Following the design of laparoscopic surgical instruments there is a trend to move from 'rigid' laparoscopic modalities to 'steerable' ones. Examples are the use of tethered drop-in detectors for US [153, 154], gamma-tracing [155], beta-tracing [156].

Trends in digital surgery

The use of target-specific contrast agents and advanced interventional modalities aligns nicely with the promising new sub-discipline of digital surgery. The concept behind digital surgery joins the power of robotics, world class instrumentation, advanced imaging and visualization, data and analytics. One may argue that an ideal procedural work flow would constitute of: 1) preoperative target assessment, 2) intraoperative navigation towards the target, and 3) intraoperative confirmation of the target location and margins [157]. A way to realize integration between these elements is through the digitization of the signals and the use of dedicated algorithms to align and interpret complementary outputs (Fig. 6).

One key aspect is the direct registration of preoperative imaging information onto the surgical field in the OR. Here, registration can take place based on endogenous structures or exogenous fiducials (also called markers). The most straight forward implementation of such registration concepts is surgical navigation, meaning that the operating surgeon can position the surgical instruments in the geographic context of preoperative images [158]. This approach is thoroughly embedded in interventions on rigid anatomies, e.g., orthopedic-, neuro- and head-and-neck surgery [22, 159, 160]. Navigation is used, for example, to guide the placement of patient tailored 3D-printed prostheses in pelvic reconstructive surgery [161]. In recent years, the concept of intraoperative navigation has been extended to soft-tissue interventions [162, 163]. However, in these soft-tissue applications realtime intraoperative imaging and therefore other modalities, such as US [164, 165], gamma probes [166] and/or fluorescence imaging [167, 168], are required to confirm the accuracy of the intraoperative navigation process.

Alternative to registration of preoperative images to the patient, intraoperative tracking and interventional modalities using exogenous fiducials, can help register the output of an imaging modality to a specific anatomical location in the patient; a concept used to generate so-called freehand scans. Freehand options have been reported for US [169], beta particles [170], gamma-ray [171], fluorescence [172], and magnetic signals [173], and have been utilized in both open and laparoscopic/robotic surgery [174]. Unique for open surgery applications is
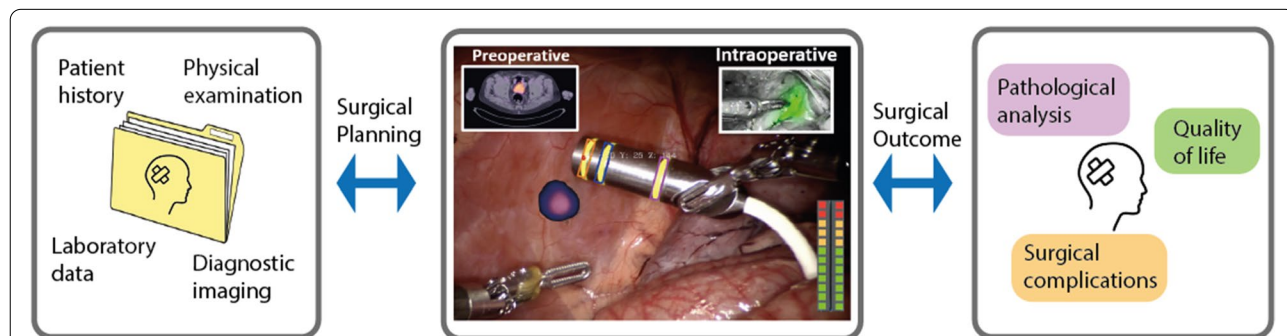
Fig. 6 Schematic explanation of the workflow in a digitally enriched surgery. Starting with the input of patient data for surgical planning. Followed by the execution of the digitally enriched surgery, including input of preoperative and intraoperative scans, tool tracking and navigation towards the target. Afterwards the surgical outcome is assessed on pathological analysis, surgical complications and if/how much the quality of life has been impacted

Boekestijn *et al. Cancer Imaging*   (2022) 22:48

Page 9 of 15

that larger detectors can be used (e.g., hand-held gamma cameras [175]) and that the rotational movement in general allows for better coverage. Uniquely, the use of a 'drop-in' gamma probe has allowed for freehand SPECT to be performed using a robotic platform [176]. A big advantage of freehand scans is that they make an overview of the situation that is encountered in the surgical setting. A downside, however, is that such scans are generally lower in quality and are often analyzed by the surgeons rather than expert radiologists or nuclear medicine physicians.

Another, perhaps more obvious, aspect of digital surgery is related to computer visualization applications. Such techniques help improve the interpretation of imaging data [177]. Intraoperatively, use of computer visualization predominantly extends the use of imaging modalities such as CT, US, gamma- and fluorescence cameras. Hereby dedicated algorithms can help enhance feature extraction and/or interpretation. A key example is the visualization of (NIR) fluorescence signals in artificial colors to improve contrast: white [178], blue [179], pink [180], or as rainbow coloration [181] whereby green (color for which the human eye is most sensitive) has been most abundantly used. Alternatively, signal intensities can be boosted digitally, where again examples can be found in fluorescence imaging [106]. A more advanced version of computer visualization is automated feature extraction and data quantification. Feature extraction can help simplify surgical and/or pathological tissue interpretations [182], but at the same time can be used to drive kinematic assessments of instrument movements [183].

While application of artificial intelligence in the realm of image-guided surgery is still limited [184], it is highly likely that such efforts will intensify in the future. In fact, this is an area where we can expect a significant impact over the coming years.

Future prospects

Clinical translation of novel image-guided surgery technologies beyond research and development requires establishment of an evidence-base that demonstrates the safety and effectiveness of these procedures, while reimbursement requires evaluation of cost-effectiveness. Strictly speaking, image-guided surgery technologies need to provide either better outcome for the patient or improve the workflow for medical professionals, if not both, and at a reasonable cost. In this regard, patient benefit can be scored by looking at short-term complication rates and long-term outcomes across cohorts with and without use of image guidance. Unfortunately, availability of such data is limited as most studies seem to focus on proof-of-principle studies. Exceptions to the rule are represented by reports for 5-ALA [185], sentinel node procedures in melanoma patients [186], ICG-^{99m}Tc-nanocolloid [48, 187, 188], and ^{99m}Tc-PSMA-I&S [189, 190]. Assessment of the impact of implementing image-guidance on surgical procedural performance, is traditionally performed via use of qualitative questionnaires and the recording of surgical time [191]. Conceptually, it is challenging to make objective and quantitative assessments regarding the adequacy of surgery or a surgeon's performance, since many individual factors may impact outcomes. Recently, as result of the performance-guided surgery paradigm, kinematic assessments have been put forward as a means to score the proficiency of a surgeon [192]. This approach has the potential to provide short term means to define the added value of an image-guidance technology [183]. Uniquely, assessment of the surgeon's performance based on kinematics will not only allow study of how chemical and engineering efforts enhance the surgical experience but will also allow assessment of how these approaches complement each other. Ultimately such assessments can be related to outcome data.

As image-guided surgery solutions are quite often technically challenging. In essence, ethics and regulations provide a healthy translational hurdle to protect patients, while financial aspects may also constrain development. from a practical perspective, lead compounds and detection device prototypes must be developed and refined in research setting and often not within the domain of patient care. While this helps preventing the patient exposure to potentially harmful technologies, it also means that some approaches can become more 'technology-driven' than 'clinical-need-driven'. Ideally all developments should be done with clinical translation in mind and based on real-life unmet surgical needs. But even with these prerequisites, it is extremely challenging to translate laboratory findings to the clinic. An example of the challenges faced is the extrapolation of findings in small animal disease-models to patients. Besides the obvious anatomical differences, which will reflect on tracer pharmacokinetics, the performance characteristics of modalities employed in small animals are not necessarily recapitulated in human instrumentation [50]. Regularly, images depicting surgery in mice that claim translational potential are published, but one should perhaps approach such claims with healthy skepticism. Phantoms can provide a size matched intermediate to test modalities on, but at the same time these settings are even more artificial than small animal disease models. This leaves large animal models like those used for surgical training purposes [180] as prime candidates for assessment of clinical potential of novel intraoperative imaging approaches. In large animals, the same type of

Boekestijn *et al. Cancer Imaging*   (2022) 22:48

Page 10 of 15

tracers, modalities or software solutions can be used as are used in patients (note: devices used on animals can no longer be used for clinical purposes). These can then also be validated in a surgical environment that is close to the intended use. A limitation is that large animal surgical-training-models are less suited as disease models as creation of such models is a costly and time-consuming ordeal that raises several ethical issues. An approach that can provide a solution from a technical perspective but at the same time demands ethical considerations is the emerging possibility wherein companion animals with cancer become potential subjects for new technology assessments [193]. An example can be found in in dogs with naturally acquired tumors [194]. Together, it seems likely that both small- and large-animal evaluations are needed to best prepare an image guidance technology for clinical evaluation. Such evaluations, combined with toxicity testing, will gather the evidence needed to apply for ethical approval for first-in-human evaluations.

Clinically surgical tasks are divided according to anatomy, disease indication and even the type of surgical intervention. This helps ensure expertise for surgeons and helps create some form of quality assurance from a healthcare perspective. From a technological perspective, however, most of these boundaries seem irrelevant. Physical and technical factors (e.g., open vs laparoscopic, soft tissue vs rigid anatomies) drives the design of new technologies. That said, most chemical and engineering efforts mentioned above still find applications in multiple settings. The success stories in the field of image-guided surgery are based on technologies that maximally align with innovations made in other fields. For example, initial work on fluorescence laparoscopy presented in prostate cancer surgery [195] was later transferred to breast surgery [196] and the technique is now also implemented during i.e., laparoscopic colorectal surgery [94, 197]. Such knowledge sharing can be considered highly valuable as it helps boost innovation across disciplines.

Conclusion

With all the promising technologies being developed under the umbrella of image-guided surgery, it remains essential to maintain a helicopter view of this highly multidisciplinary and rapidly expanding field. Hereby, we need to make sure that the clinical needs remain aligned with tracer chemistry, device physics and the increasing digitization of the operating room.

Abbreviations

US: Ultrasound; CT: Computed tomography; MRI: Magnetic resonance imaging; PET: Positron emission tomography; PSMA: Prostate specific membrane antigen; ICG: Indocyanine green; 3D: Three-dimensional; SPECT: Single photon emission computed tomography; OR: Operating room.

Supplementary Information

Additional file 1.

Acknowledgements

Authors' contributions

Funding

Availability of data and materials
Not applicable.

Declarations

Ethics approval and consent to participate
Not applicable.

Consent for publication
Not applicable.

Competing interests
The authors declare no that they have no competing interests.

Author details
[1]Interventional Molecular Imaging Laboratory, Department of Radiology, Leiden University Medical Center, Leiden, the Netherlands. [2]Section of Nuclear Medicine, Department of Radiology, Leiden University Medical Center, Leiden, the Netherlands. [3]Department of Urology, ASST Grande Ospedale Metropolitano Niguarda, Milan, Italy. [4]Medical Physics, Department of Radiology , Leiden University Medical Center, Leiden, the Netherlands. [5]Department of Clinical Farmacy and Toxicology, Leiden University Medical Center, Leiden, the Netherlands. [6]Martini-Klinik Prostate Cancer Centre Hamburg, Hamburg, Germany.

References

1. Terreno E, Uggeri F, Aime S. Image guided therapy: The advent of theranostic agents. J Control Release. 2012;161(2):328–37.
2. Gupta S, Madoff DC. Image-Guided Percutaneous Needle Biopsy in Cancer Diagnosis and Staging. Tech Vasc Interv Radiol. 2007;10(2):88–101.
3. Rammohan A, Sathyanesan J, Ramaswami S, Lakshmanan A, Senthil-Kumar P, Srinivasan UP, et al. Embolization of liver tumors: Past, present and future. World J Radiol. 2012;4(9):405–12.
4. Roh HF, Nam SH, Kim JM. Robot-assisted laparoscopic surgery versus conventional laparoscopic surgery in randomized controlled trials: A systematic review and meta-analysis. PLoS ONE. 2018;13(1): e0191628.
5. Ficarra V, Cavalleri S, Novara G, Aragona M, Artibani W. Evidence from Robot-Assisted Laparoscopic Radical Prostatectomy: A Systematic Review. Eur Urol. 2007;51(1):45–56.
6. Estey EP. Robotic prostatectomy: The new standard of care or a marketing success? Can Urol Assoc J. 2009;3(6):488–90.

7. Cleary K, Peters TM. Image-Guided Interventions: Technology Review and Clinical Applications. Annu Rev Biomed Eng. 2010;12(1):119–42.

8. Azagury DE, Dua MM, Barrese JC, Henderson JM, Buchs NC, Ris F, et al. Image-guided surgery. Curr Probl Surg. 2015;52(12):476–520.

9. Boni L, David G, Mangano A, Dionigi G, Rausei S, Spampatti S, et al. Clinical applications of indocyanine green (ICG) enhanced fluorescence in laparoscopic surgery. Surg Endosc. 2015;29(7):2046–55.

10. Tanaka E, Choi HS, Fujii H, Bawendi MG, Frangioni JV. Image-Guided Oncologic Surgery Using Invisible Light: Completed Pre-Clinical Development for Sentinel Lymph Node Mapping. Ann Surg Oncol. 2006;13(12):1671–81.

11. Thomas TP, Myaing MT, Ye JY, Candido K, Kotlyar A, Beals J, et al. Detection and analysis of tumor fluorescence using a two-photon optical fiber probe. Biophys J. 2004;86(6):3959–65.

12. Székely G, Nolte L-P. Image guidance in orthopaedics and traumatology: A historical perspective. Med Image Anal. 2016;33:79–83.

13. Makuuchi M, Torzilli G, Machi J. History of intraoperative ultrasound. Ultrasound Med Biol. 1998;24(9):1229–42.

14. Schlag PM. The 'Sentinel Node' Concept: More Questions Raised than Answers Provided? Oncologist. 1998;3(5):Vi-vii.

15. Wawroschek F, Vogt H, Weckermann D, Wagner T, Harzmann R. The Sentinel Lymph Node Concept in Prostate Cancer – First Results of Gamma Probe-Guided Sentinel Lymph Node Identification. Eur Urol. 1999;36(6):595–600.

16. Krenning EP, Kwekkeboom DJ, Bakker WH, Breeman WA, Kooij PP, Oei HY, et al. Somatostatin receptor scintigraphy with [111In-DTPA-D-Phe1]- and [123I-Tyr3]-octreotide: the Rotterdam experience with more than 1000 patients. Eur J Nucl Med. 1993;20(8):716–31.

17. Black PM, Moriarty T, Alexander E, Stieg P, Woodard EJ, Gleason PL, et al. Development and Implementation of Intraoperative Magnetic Resonance Imaging and Its Neurosurgical Applications. Neurosurgery. 1997;41(4):831–45.

18. Winter A, Engels S, Wawroschek F. Sentinel lymph node surgery in prostate cancer using magnetic particles. Curr Opin Urol. 2018;28(2):184–90.

19. Birkhäuser FD, Studer UE, Froehlich JM, Triantafyllou M, Bains LJ, Petralia G, et al. Combined Ultrasmall Superparamagnetic Particles of Iron Oxide-Enhanced and Diffusion-weighted Magnetic Resonance Imaging Facilitates Detection of Metastases in Normal-sized Pelvic Lymph Nodes of Patients with Bladder and Prostate Cancer. Eur Urol. 2013;64(6):953–60.

20. de Boer E, Harlaar NJ, Taruttis A, Nagengast WB, Rosenthal EL, Ntziachristos V, et al. Optical innovations in surgery. Br J Surg. 2015;102(2):e56–72.

21. Keereweer S, Kerrebijn JDF, van Driel PBAA, Xie B, Kaijzel EL, Snoeks TJA, et al. Optical Image-guided Surgery—Where Do We Stand? Mol Imag Biol. 2011;13(2):199–207.

22. Mezger U, Jendrewski C, Bartels M. Navigation in surgery. Langenbecks Arch Surg. 2013;398(4):501–14.

23. Maecke HR, Reubi JC. Somatostatin Receptors as Targets for Nuclear Medicine Imaging and Radionuclide Treatment. J Nucl Med. 2011;52(6):841–4.

24. Demirci E, Sahin OE, Ocak M, Akovali B, Nematyazar J, Kabasakal L. Normal distribution pattern and physiological variants of 68Ga-PSMA-11 PET/CT imaging. Nucl Med Commun. 2016;37(11):1169–7.

25. Ewelt C, Nemes A, Senner V, Wölfer J, Brokinkel B, Stummer W, et al. Fluorescence in neurosurgery: Its diagnostic and therapeutic use. Review of the literature. J Photochem Photobiol B. 2015;148:302–9.

26. Darmoch F, Alraies MC, Al-Khadra Y, Moussa Pacha H, Pinto DS, Osborn EA. Intravascular ultrasound imaging–guided versus coronary angiography–guided percutaneous coronary intervention: a systematic review and meta-analysis. J Am Heart Assoc. 2020;9(5): e013678.

27. Tacher V, Lin M, Desgranges P, Deux J-F, Grünhagen T, Becquemin J-P, et al. Image Guidance for Endovascular Repair of Complex Aortic Aneurysms: Comparison of Two-dimensional and Three-dimensional Angiography and Image Fusion. J Vasc Interv Radiol. 2013;24(11):1698–706.

28. Ankersmit M, van Dam DA, van Rijswijk AS, van den Heuvel B, Tuynman JB, Meijerink W. Fluorescent Imaging With Indocyanine Green During Laparoscopic Cholecystectomy in Patients at Increased Risk of Bile Duct Injury. Surg Innov. 2017;24(3):245–52.

29. Ladurner R, Lerchenberger M, Al Arabi N, Gallwas JKS, Stepp H, Hallfeldt KKJ. Parathyroid Autofluorescence-How Does It Affect Parathyroid and Thyroid Surgery? A 5 Year Experience. Molecules. 2019;24(14):2560.

30. Wang B, Zhu C-R, Liu H, Yao X-M, Wu J. The Accuracy of Near Infrared Autofluorescence in Identifying Parathyroid Gland During Thyroid and Parathyroid Surgery: A Meta-Analysis. Frontiers in Endocrinology. 2021;12(764).

31. Marshall MV, Rasmussen JC, Tan IC, Aldrich MB, Adams KE, Wang X, et al. Near-Infrared Fluorescence Imaging in Humans with Indocyanine Green: A Review and Update. Open Surg Oncol J. 2010;2(2):12–25.

32. Lee ES, Kim TS, Kim S-K. Current Status of Optical Imaging for Evaluating Lymph Nodes and Lymphatic System. kjr. 2015;16(1):21–31.

33. Rafferty MA, Siewerdsen JH, Chan Y, Daly MJ, Moseley DJ, Jaffray DA, et al. Intraoperative Cone-beam CT for Guidance of Temporal Bone Surgery. Otolaryngology-Head and Neck Surgery. 2006;134(5):801–8.

34. Tsuchiya Y. Early carcinoma of the gallbladder: macroscopic features and US findings. Radiology. 1991;179(1):171–5.

35. Sanai N, Snyder LA, Honea NJ, Coons SW, Eschbacher JM, Smith KA, et al. Intraoperative confocal microscopy in the visualization of 5-aminolevulinic acid fluorescence in low-grade gliomas: Clinical article. J Neurosurg. 2011;115(4):740–8.

36. Meershoek P, Buckle T, van Oosterom MN, KleinJan GH, van der Poel HG, van Leeuwen FWB. Can Intraoperative Fluorescence Imaging Identify All Lesions While the Road Map Created by Preoperative Nuclear Imaging Is Masked? J Nucl Med. 2020;61(6):834–41.

37. Jeschke S, Lusuardi L, Myatt A, Hruby S, Pirich C, Janetschek G. Visualisation of the lymph node pathway in real time by laparoscopic radioisotope- and fluorescence-guided sentinel lymph node dissection in prostate cancer staging. Urology. 2012;80(5):1080–6.

38. Mohajerani P, Tzoumas S, Rosenthal A, Ntziachristos V. Optical and Optoacoustic Model-Based Tomography: Theory and current challenges for deep tissue imaging of optical contrast. IEEE Signal Process Mag. 2015;32(1):88–100.

39. Dhawan AP, Alessandro BD, Fu X. Optical Imaging Modalities for Biomedical Applications. IEEE Rev Biomed Eng. 2010;3:69–92.

40. Robu S, Schottelius M, Eiber M, Maurer T, Gschwend J, Schwaiger M, et al. Preclinical Evaluation and First Patient Application of 99mTc-PSMA-I&S for SPECT Imaging and Radioguided Surgery in Prostate Cancer. J Nucl Med. 2017;58(2):235–42.

41. van Leeuwen FWB, Winter A, van Der Poel HG, Eiber M, Suardi N, Graefen M, et al. Technologies for image-guided surgery for managing lymphatic metastases in prostate cancer. Nat Rev Urol. 2019;16(3):159–71.

42. Goyal A, Newcombe RG, Mansel RE. Role of routine preoperative lymphoscintigraphy in sentinel node biopsy for breast cancer. Eur J Cancer. 2005;41(2):238–43.

43. Vermeeren L, van der Ploeg IM, Olmos RA, Meinhardt W, Klop WM, Kroon BB, et al. SPECT/CT for preoperative sentinel node localization. J Surg Oncol. 2010;101(2):184–90.

44. Miracle AC, Mukherji SK. Conebeam CT of the Head and Neck, Part 2: Clinical Applications. Am J Neuroradiol. 2009;30(7):1285–92.

45. Kubben PL, ter Meulen KJ, Schijns OEMG, ter Laak-Poort MP, van Overbeeke JJ, Santbrink Hv. Intraoperative MRI-guided resection of glioblastoma multiforme: a systematic review. The Lancet Oncology. 2011;12(11):1062–70.

46. van Leeuwen FW, Hardwick JC, van Erkel AR. Luminescence-based Imaging Approaches in the Field of Interventional Molecular Imaging. Radiology. 2015;276(1):12–29.

47. Hricak H, Choi BI, Scott AM, Sugimura K, Muellner A, Schulthess GKv, et al. Global Trends in Hybrid Imaging. Radiology. 2010;257(2):498–506.

48. Dell'Oglio P, de Vries HM, Mazzone E, KleinJan GH, Donswijk ML, van der Poel HG, et al. Hybrid Indocyanine Green-(99m)Tc-nanocolloid for Single-photon Emission Computed Tomography and Combined Radio- and Fluorescence-guided Sentinel Node Biopsy in Penile Cancer: Results of 740 Inguinal Basins Assessed at a Single Institution. Eur Urol. 2020;78(6):865–72.

49. Achilefu S. Introduction to Concepts and Strategies for Molecular Imaging. Chem Rev. 2010;110(5):2575–8.

50. van Leeuwen FWB, Schottelius M, Brouwer OR, Vidal-Sicart S, Achilefu S, Klode J, et al. Trending: Radioactive and Fluorescent Bimodal/Hybrid Tracers as Multiplexing Solutions for Surgical Guidance. J Nucl Med. 2020;61(1):13–9.

51. Van Den Berg NS, Buckle T, Kleinjan GI, Klop WM, Horenblas S, Van Der Poel HG, et al. Hybrid tracers for sentinel node biopsy. Q J Nucl Med Mol Imaging. 2014;58(2):193–206.

Boekestijn *et al. Cancer Imaging*   (2022) 22:48

Page 12 of 15

52. Wang S, Yang W, Deng J, Zhang J, Ma F, Wang J. Reduction in the recurrence of meningiomas by combining somatostatin receptor scintigraphy of (99m)Tc-HYNIC-octreotide SPECT/CT and radio guidance with a hand-held γ-probe during surgery. Nucl Med Commun. 2013;34(3):249–53.

53. Cuccurullo V, Di Stasio GD, Mansi L. Radioguided surgery with radiolabeled somatostatin analogs: not only in GEP-NETs. Nuclear Medicine Review. 2017;20(1):49–56.

54. Hensbergen AW, van Willigen DM, van Beurden F, van Leeuwen PJ, Buckle T, Schottelius M, et al. Image-Guided Surgery: Are We Getting the Most Out of Small-Molecule Prostate-Specific-Membrane-Antigen-Targeted Tracers? Bioconjug Chem. 2020;31(2):375–95.

55. Bunschoten A, van den Berg NS, Valdés Olmos RA, Blokland JAK, van Leeuwen FWB. Tracers Applied in Radioguided Surgery. In: Herrmann K, Nieweg OE, Povoski SP, editors. Radioguided Surgery: Current Applications and Innovative Directions in Clinical Practice. Cham: Springer International Publishing; 2016. p. 75–101.

56. Maurer T, Robu S, Schottelius M, Schwamborn K, Rauscher I, van den Berg NS, et al. [99m]Technetium-based Prostate-specific Membrane Antigen–radioguided Surgery in Recurrent Prostate Cancer. Eur Urol. 2019;75(4):659–66.

57. Graham MM. Clinical Molecular Imaging with Radiotracers: Current Status. Med Princ Pract. 2012;21(3):197–208.

58. Cazzato RL, Garnon J, Shaygi B, Koch G, Tsoumakidou G, Caudrelier J, et al. PET/CT-guided interventions: Indications, advantages, disadvantages and the state of the art. Minim Invasive Ther Allied Technol. 2018;27(1):27–32.

59. Collamati F, Maccora D, Alfieri S, Bocci V, Cartoni A, Collarino A, et al. Radioguided surgery with β(-) radiation in pancreatic Neuroendocrine Tumors: a feasibility study. Sci Rep. 2020;10(1):4015.

60. Das S, Thorek DL, Grimm J. Cerenkov imaging. Adv Cancer Res. 2014;124:213–34.

61. Vallée JP, Lazeyras F, Khan HG, Terrier F. Absolute renal blood flow quantification by dynamic MRI and Gd-DTPA. Eur Radiol. 2000;10(8):1245–52.

62. Cademartiri F, de Monye C, Pugliese F, Mollet NR, Runza G, van der Lugt A, et al. High Iodine Concentration Contrast Material for Noninvasive Multislice Computed Tomography Coronary Angiography: Iopromide 370 Versus Iomeprol 400. Invest Radiol. 2006;41(3):349–53.

63. Ichihara M, Sasaki K, Umemura S-I, Kushima M, Okai T. Blood Flow Occlusion Via Ultrasound Image-Guided High-Intensity Focused Ultrasound and Its Effect on Tissue Perfusion. Ultrasound Med Biol. 2007;33(3):452–9.

64. Yamamoto M, Sasaguri S, Sato T. Assessing intraoperative blood flow in cardiovascular surgery. Surg Today. 2011;41(11):1467.

65. Spaide RF, Klancnik JM Jr, Cooney MJ. Retinal Vascular Layers Imaged by Fluorescein Angiography and Optical Coherence Tomography Angiography. JAMA Ophthalmology. 2015;133(1):45–50.

66. Vidal-Sicart S, van Leeuwen FWB, van den Berg NS, Valdés Olmos RA. Fluorescent radiocolloids: are hybrid tracers the future for lymphatic mapping? Eur J Nucl Med Mol I. 2015;42(11):1627–30.

67. Winter A, Kowald T, Engels S, Wawroschek F. Magnetic Resonance Sentinel Lymph Node Imaging and Magnetometer-Guided Intraoperative Detection in Penile Cancer, using Superparamagnetic Iron Oxide Nanoparticles: First Results. Urol Int. 2020;104(3–4):177–80.

68. Valiveru RC, Agarwal G, Agrawal V, Gambhir S, Mayilvaganan S, Chand G, et al. Low-cost Fluorescein as an Alternative to Radio-colloid for Sentinel Lymph Node Biopsy—a Prospective Validation Study in Early Breast Cancer. World J Surg. 2020;44(10):3417–22.

69. de Graaf W, van Lienden KP, van Gulik TM, Bennink RJ. (99m)Tc-mebrofenin hepatobiliary scintigraphy with SPECT for the assessment of hepatic function and liver functional volume before partial hepatectomy. J Nucl Med. 2010;51(2):229–36.

70. Pfeifer N, Goss S, Swift B, Ghibellini G, Ivanovic M, Heizer W, et al. Effect of Ritonavir on 99mTechnetium–Mebrofenin Disposition in Humans: A Semi-PBPK Modeling and In Vitro Approach to Predict Transporter-Mediated DDIs. CPT: Pharmacometrics & Systems Pharmacology. 2013;2(1):20.

71. Uesaka K, Nimura Y, Nagino M. Changes in hepatic lobar function after right portal vein embolization. An appraisal by biliary indocyanine green excretion. Ann Surg. 1996;223(1):77–83.

72. Giovanella L, Avram AM, Iakovou I, Kwak J, Lawson SA, Lulaj E, et al. EANM practice guideline/SNMMI procedure standard for RAIU and thyroid scintigraphy. Eur J Nucl Med Mol I. 2019;46(12):2514–25.

73. Strauss SB, Roytman M, Phillips CD. Parathyroid Imaging: Four-dimensional Computed Tomography, Sestamibi, and Ultrasonography. Neuroimaging Clin N Am. 2021;31(3):379–95.

74. Sandqvist P, Nilsson I-L, Grybäck P, Sanchez-Crespo A, Sundin A. Multiphase Iodine Contrast-Enhanced SPECT/CT Outperforms Nonenhanced SPECT/CT for Preoperative Localization of Small Parathyroid Adenomas. Clin Nucl Med. 2019;44(12):929–35.

75. Zaidi N, Bucak E, Okoh A, Yazici P, Yigitbas H, Berber E. The utility of indocyanine green near infrared fluorescent imaging in the identification of parathyroid glands during surgery for primary hyperparathyroidism. J Surg Oncol. 2016;113(7):771–4.

76. Mariani G, Gulec SA, Rubello D, Boni G, Puccini M, Pelizzo MR, et al. Preoperative Localization and Radioguided Parathyroid Surgery. J Nucl Med. 2003;44(9):1443–58.

77. KleinJan GH, Bunschoten A, Brouwer OR, van den Berg NS, Valdés-Olmos RA, van Leeuwen FWB. Multimodal imaging in radioguided surgery. Clinical and Translational Imaging. 2013;1(6):433–44.

78. Owens J, Bolster AA, Prosser JE, Cunningham S, Mairs RJ, Neilly JB, et al. No-carrier-added 123I-MIBG: An initial clinical study in patients with phaeochromocytoma. Nuclear Medicine Communications. 2000;21(5).

79. Hadjipanayis CG, Stummer W. 5-ALA and FDA approval for glioma surgery. J Neurooncol. 2019;141(3):479–86.

80. Celli JP, Spring BQ, Rizvi I, Evans CL, Samkoe KS, Verma S, et al. Imaging and photodynamic therapy: mechanisms, monitoring, and optimization. Chem Rev. 2010;110(5):2795–838.

81. Lapini A, Minervini A, Masala A, Schips L, Pycha A, Cindolo L, et al. A comparison of hexaminolevulinate (Hexvix(®)) fluorescence cystoscopy and white-light cystoscopy for detection of bladder cancer: results of the HeRo observational study. Surg Endosc. 2012;26(12):3634–41.

82. Ricard M, Tenenbaum F, Schlumberger M, Travagli JP, Lumbroso J, Revillon Y, et al. Intraoperative detection of pheochromocytoma with iodine-125 labelled meta-iodobenzylguanidine: a feasibility study. Eur J Nucl Med. 1993;20(5):426–30.

83. Sandgren K, Johansson L, Axelsson J, Jonsson J, Ögren M, Ögren M, et al. Radiation dosimetry of [(68)Ga]PSMA-11 in low-risk prostate cancer patients. EJNMMI Phys. 2019;6(1):2.

84. Giesel FL, Knorr K, Spohn F, Will L, Maurer T, Flechsig P, et al. Detection Efficacy of ^{18}F-PSMA-1007 PET/CT in 251 Patients with Biochemical Recurrence of Prostate Cancer After Radical Prostatectomy. J Nucl Med. 2019;60(3):362–8.

85. Maurer T, Weirich G, Schottelius M, Weineisen M, Frisch B, Okur A, et al. Prostate-specific Membrane Antigen–radioguided Surgery for Metastatic Lymph Nodes in Prostate Cancer. Eur Urol. 2015;68(3):530–4.

86. Eder AC, Omrane MA, Stadlbauer S, Roscher M, Khoder WY, Gratzke C, et al. The PSMA-11-derived hybrid molecule PSMA-914 specifically identifies prostate cancer by preoperative PET/CT and intraoperative fluorescence imaging. Eur J Nucl Med Mol Imaging. 2021;48(6):2057–8.

87. Hofmann M, Maecke H, Börner A, Weckesser E, Schöffski P, Oei M, et al. Biokinetics and imaging with the somatostatin receptor PET radioligand 68Ga-DOTATOC: preliminary data. Eur J Nucl Med. 2001;28(12):1751–7.

88. Graham MM, Gu X, Ginader T, Breheny P, Sunderland JJ. (68)Ga-DOTA-TOC Imaging of Neuroendocrine Tumors: A Systematic Review and Metaanalysis. J Nucl Med. 2017;58(9):1452–8.

89. Krenning EP, Kwekkeboom DJ, Bakker WH, Breeman WAP, Kooij PPM, Oei HY, et al. Somatostatin receptor scintigraphy with [111In-DTPA-d-Phe1]- and [123I-Tyr3]-octreotide: the Rotterdam experience with more than 1000 patients. Eur J Nucl Med. 1993;20(8):716–31.

90. Van Den Bossche B, D'haeninck E, De Vos F, Dierckx RA, Van Belle S, Bracke M, et al. Oestrogen-mediated regulation of somatostatin receptor expression in human breast cancer cell lines assessed with 99mTc-depreotide. Eur J Nucl Med Mol I. 2004;31(7):1022–30.

91. Yamaga LYI, Cunha ML, Campos Neto GC, Garcia MRT, Yang JH, Camacho CP, et al. (68)Ga-DOTATATE PET/CT in recurrent medullary thyroid carcinoma: a lesion-by-lesion comparison with (111)In-octreotide SPECT/CT and conventional imaging. Eur J Nucl Med Mol Imaging. 2017;44(10):1695–701.

Boekestijn *et al. Cancer Imaging*　　(2022) 22:48

Page 13 of 15

92. Mittlmeier LM, Todica A, Gildehaus F-J, Unterrainer M, Beyer L, Brendel M, et al. 68Ga-EMP-100 PET/CT—a novel ligand for visualizing c-MET expression in metastatic renal cell carcinoma—first in-human biodistribution and imaging results. Eur J Nucl Med Mol I. 2021.

93. de Jongh SJ, Vrouwe JPM, Voskuil FJ, Schmidt I, Westerhof J, Koornstra JJ, et al. The Optimal Imaging Window for Dysplastic Colorectal Polyp Detection Using c-Met–Targeted Fluorescence Molecular Endoscopy. J Nucl Med. 2020;61(10):1435–41.

94. Burggraaf J, Kamerling IM, Gordon PB, Schrier L, de Kam ML, Kales AJ, et al. Detection of colorectal polyps in humans using an intravenously administered fluorescent peptide targeted against c-Met. Nat Med. 2015;21(8):955–61.

95. Kang F, Wang Z, Li G, Wang S, Liu D, Zhang M, et al. Inter-heterogeneity and intra-heterogeneity of αvβ3 in non-small cell lung cancer and small cell lung cancer patients as revealed by 68Ga-RGD2 PET imaging. Eur J Nucl Med Mol I. 2017;44(9):1520–8.

96. Li L, Zhao W, Sun X, Liu N, Zhou Y, Luan X, et al. (18)F-RGD PET/CT imaging reveals characteristics of angiogenesis in non-small cell lung cancer. Transl Lung Cancer Res. 2020;9(4):1324–32.

97. Handgraaf HJM, Boonstra MC, Prevoo H, Kuil J, Bordo MW, Boogerd LSF, et al. Real-time near-infrared fluorescence imaging using cRGD-ZW800-1 for intraoperative visualization of multiple cancer types. Oncotarget. 2017;8(13):21054–66.

98. Phillips E, Penate-Medina O, Zanzonico PB, Carvajal RD, Mohan P, Ye Y, et al. Clinical translation of an ultrasmall inorganic optical-PET imaging nanoparticle probe. Sci Transl Med. 2014;6(260):260ra149.

99. Bahce I, Huisman MC, Verwer EE, Ooijevaar R, Boutkourt F, Vugts DJ, et al. Pilot study of 89Zr-bevacizumab positron emission tomography in patients with advanced non-small cell lung cancer. EJNMMI Res. 2014;4(1):35.

100. Lamberts LE, Koch M, de Jong JS, Adams ALL, Glatz J, Kranendonk MEG, et al. Tumor-Specific Uptake of Fluorescent Bevacizumab-IRDye800CW Microdosing in Patients with Primary Breast Cancer: A Phase I Feasibility Study. Clin Cancer Res. 2017;23(11):2730–41.

101. Keyaerts M, Xavier C, Heemskerk J, Devoogdt N, Everaert H, Ackaert C, et al. Phase I Study of 68Ga-HER2-Nanobody for PET/CT Assessment of HER2 Expression in Breast Carcinoma. J Nucl Med. 2016;57(1):27–33.

102. Kijanka M, Warnders F-J, El Khattabi M, Lub-de Hooge M, van Dam GM, Ntziachristos V, et al. Rapid optical imaging of human breast tumour xenografts using anti-HER2 VHHs site-directly conjugated to IRDye 800CW for image-guided surgery. Eur J Nucl Med Mol I. 2013;40(11):1718–29.

103. Sampath L, Kwon S, Ke S, Wang W, Schiff R, Mawad ME, et al. Dual-labeled trastuzumab-based imaging agent for the detection of human epidermal growth factor receptor 2 overexpression in breast cancer. J Nucl Med. 2007;48(9):1501–10.

104. de Gooyer JM, Elekonawo FMK, Bos DL, van der Post RS, Pèlegrin A, Framery B, et al. Multimodal CEA-Targeted Image-Guided Colorectal Cancer Surgery using ¹¹¹In-Labeled SGM-101. Clin Cancer Res. 2020;26(22):5934–42.

105. Elekonawo FMK, Lütje S, Franssen GM, Bos DL, Goldenberg DM, Boerman OC, et al. A pretargeted multimodal approach for image-guided resection in a xenograft model of colorectal cancer. EJNMMI Res. 2019;9(1):86.

106. Meershoek P, KleinJan GH, van Willigen DM, Bauwens KP, Spa SJ, van Beurden F, et al. Multi-wavelength fluorescence imaging with a da Vinci Firefly—a technical look behind the scenes. J Robot Surg. 2021;15(5):751–60.

107. Hoogstins CES, Boogerd LSF, Sibinga Mulder BG, Mieog JSD, Swijnenburg RJ, van de Velde CJH, et al. Image-Guided Surgery in Patients with Pancreatic Cancer: First Results of a Clinical Trial Using SGM-101, a Novel Carcinoembryonic Antigen-Targeting. Near-Infrared Fluorescent Agent Ann Surg Oncol. 2018;25(11):3350–7.

108. Folli S, Wagnières G, Pèlegrin A, Calmes JM, Braichotte D, Buchegger F, et al. Immunophotodiagnosis of colon carcinomas in patients injected with fluoresceinated chimeric antibodies against carcinoembryonic antigen. Proc Natl Acad Sci U S A. 1992;89(17):7973–7.

109. Menke-van der Houven van Oordt CW, Gootjes EC, Huisman MC, Vugts DJ, Roth C, Luik AM, et al. 89Zr-cetuximab PET imaging in patients with advanced colorectal cancer. Oncotarget. 2015;6(30):30384–93.

110. Tummers WS, Miller SE, Teraphongphom NT, Gomez A, Steinberg I, Huland DM, et al. Intraoperative Pancreatic Cancer Detection using Tumor-Specific Multimodality Molecular Imaging. Ann Surg Oncol. 2018;25(7):1880–8.

111. Tummers WS, Miller SE, Teraphongphom NT, van den Berg NS, Hasan A, Longacre TA, et al. Detection of visually occult metastatic lymph nodes using molecularly targeted fluorescent imaging during surgical resection of pancreatic cancer. HPB (Oxford). 2019;21(7):883–90.

112. Miller SE, Tummers WS, Teraphongphom N, van den Berg NS, Hasan A, Ertsey RD, et al. First-in-human intraoperative near-infrared fluorescence imaging of glioblastoma using cetuximab-IRDye800. J Neurooncol. 2018;139(1):135–43.

113. van Keulen S, van den Berg NS, Nishio N, Birkeland A, Zhou Q, Lu G, et al. Rapid, non-invasive fluorescence margin assessment: Optical specimen mapping in oral squamous cell carcinoma. Oral Oncol. 2019;88:58–65.

114. Hekman MCH, Rijpkema M, Aarntzen EH, Mulder SF, Langenhuijsen JF, Oosterwijk E, et al. Positron Emission Tomography/Computed Tomography with 89Zr-girentuximab Can Aid in Diagnostic Dilemmas of Clear Cell Renal Cell Carcinoma Suspicion. Eur Urol. 2018;74(3):257–60.

115. Khandani AH, Rathmell WK. Positron Emission Tomography in Renal Cell Carcinoma: An Imaging Biomarker in Development. Semin Nucl Med. 2012;42(4):221–30.

116. Hekman MC, Rijpkema M, Muselaers CH, Oosterwijk E, Hulsbergen-Van de Kaa CA, Boerman OC, et al. Tumor-targeted Dual-modality Imaging to Improve Intraoperative Visualization of Clear Cell Renal Cell Carcinoma: A First in Man Study. Theranostics. 2018;8(8):2161–70.

117. Nguyen QT, Tsien RY. Fluorescence-guided surgery with live molecular navigation — a new cutting edge. Nat Rev Cancer. 2013;13(9):653–62.

118. van Beurden F, van Willigen DM, Vojnovic B, van Oosterom MN, Brouwer OR, der Poel HGV, et al. Multi-Wavelength Fluorescence in Image-Guided Surgery, Clinical Feasibility and Future Perspectives. Mol Imaging. 2020;19:1536012120962333.

119. Buckle T, van Willigen DM, Spa SJ, Hensbergen AW, van der Wal S, de Korne CM, et al. Tracers for fluorescence-guided surgery: how elongation of the polymethine chain in cyanine dyes alters the pharmacokinetics of a (bimodal) c[RGDyK] tracer. Journal of Nuclear Medicine. 2018:jnumed.117.205575.

120. Debie P, Van Quathem J, Hansen I, Bala G, Massa S, Devoogdt N, et al. Effect of Dye and Conjugation Chemistry on the Biodistribution Profile of Near-Infrared-Labeled Nanobodies as Tracers for Image-Guided Surgery. Mol Pharm. 2017;14(4):1145–53.

121. Cohen R, Stammes MA, de Roos IH, Stigter-van Walsum M, Visser GW, van Dongen GA. Inert coupling of IRDye800CW to monoclonal antibodies for clinical optical imaging of tumor targets. EJNMMI Res. 2011;1(1):31.

122. Saleem A, Aboagye EO, Price PM. In vivo monitoring of drugs using radiotracer techniques. Adv Drug Deliv Rev. 2000;41(1):21–39.

123. Hensbergen AW, van Willigen DM, van Beurden F, van Leeuwen PJ, Buckle T, Schottelius M, et al. Image-Guided Surgery: Are We Getting the Most Out of Small-Molecule Prostate-Specific-Membrane-Antigen-Targeted Tracers? Bioconjug Chem. 2020;31(2):375–95.

124. Chin PTK, Welling MM, Meskers SCJ, Valdes Olmos RA, Tanke H, van Leeuwen FWB. Optical imaging as an expansion of nuclear medicine: Cerenkov-based luminescence vs fluorescence-based luminescence. Eur J Nucl Med Mol I. 2013;40(8):1283–91.

125. Kiani A, Esquevin A, Lepareur N, Bourguet P, Le Jeune F, Gauvrit J. Main applications of hybrid PET-MRI contrast agents: a review. Contrast Media Mol Imaging. 2016;11(2):92–8.

126. Van Oosterom MN, Rietbergen DDD, Welling MM, Van Der Poel HG, Maurer T, Van Leeuwen FWB. Recent advances in nuclear and hybrid detection modalities for image-guided surgery. Expert Rev Med Devices. 2019;16(8):711–34.

127. Spa SJ, Bunschoten A, Rood MT, Peters RJ, Koster AJ, van Leeuwen FW. Orthogonal Functionalization of Ferritin via Supramolecular Re-Assembly. Eur J Inorg Chem. 2015;2015(27):4603–10.

128. van der Wal S, Kuil J, Valentijn ARPM, van Leeuwen FWB. Synthesis and systematic evaluation of symmetric sulfonated centrally CC bonded cyanine near-infrared dyes for protein labelling. Dyes Pigm. 2016;132:7–19.

Boekestijn *et al. Cancer Imaging*   (2022) 22:48

Page 14 of 15

129. Cohen R, Stammes MA, de Roos IH, Stigter-van Walsum M, Visser GW, van Dongen GA. Inert coupling of IRDye800CW to monoclonal antibodies for clinical optical imaging of tumor targets. EJNMMI Res. 2011;1(1):31.

130. Pronkin P, Tatikolov A. Isomerization and Properties of Isomers of Carbocyanine Dyes. Sci. 2019;1(1):19.

131. Quan B, Choi K, Kim Y-H, Kang KW, Chung DS. Near infrared dye indocyanine green doped silica nanoparticles for biological imaging. Talanta. 2012;99:387–93.

132. Zhegalova NG, He S, Zhou H, Kim DM, Berezin MY. Minimization of self-quenching fluorescence on dyes conjugated to biomolecules with multiple labeling sites via asymmetrically charged NIR fluorophores. Contrast Media Mol Imaging. 2014;9(5):355–62.

133. Daly MJ, Siewerdsen JH, Cho YB, Jaffray DA, Irish JC. Geometric calibration of a mobile C-arm for intraoperative cone-beam CT. Med Phys. 2008;35(5):2124–36.

134. Liu WP, Richmon JD, Sorger JM, Azizian M, Taylor RH. Augmented reality and cone beam CT guidance for transoral robotic surgery. J Robot Surg. 2015;9(3):223–33.

135. Aldrich JE. Basic physics of ultrasound imaging. Crit Care Med. 2007;35(5):S131–7.

136. Zhang DY, Singhal S, Lee JYK. Optical Principles of Fluorescence-Guided Brain Tumor Surgery: A Practical Primer for the Neurosurgeon. Neurosurgery. 2018;85(3):312–24.

137. Sexton K, Davis SC, McClatchy D, Valdes PA, Kanick SC, Paulsen KD, et al. Pulsed-light imaging for fluorescence guided surgery under normal room lighting. Opt Lett. 2013;38(17):3249–52.

138. van den Berg NS, Miwa M, KleinJan GH, Sato T, Maeda Y, van Akkooi ACJ, et al. (Near-Infrared) Fluorescence-Guided Surgery Under Ambient Light Conditions: A Next Step to Embedment of the Technology in Clinical Routine. Ann Surg Oncol. 2016;23(8):2586–95.

139. van Oosterom M, den Houting D, van de Velde C, van Leeuwen F. Navigating surgical fluorescence cameras using near-infrared optical tracking. J Biomed Opt. 2018;23(5): 056003.

140. Dietze MM, Bastiaannet R, Kunnen B, van der Velden S, Lam MG, Viergever MA, et al. Respiratory motion compensation in interventional liver SPECT using simultaneous fluoroscopic and nuclear imaging. Med Phys. 2019;46(8):3496–507.

141. Vidal-Sicart S, Seva A, Campos F, Sánchez N, Alonso I, Pahisa J, et al. Clinical use of an opto-nuclear probe for hybrid sentinel node biopsy guidance: first results. Int J Comput Assist Radiol Surg. 2019;14(2):409–16.

142. Pani R, Pellegrini R, Cinti MN, Polito C, Orlandi C, Fabbri A, et al. Integrated ultrasound and gamma imaging probe for medical diagnosis. J Instrum. 2016;11(03):C03037-C.

143. Ullah MN, Park Y, Kim GB, Kim C, Park C, Choi H, et al. Simultaneous Acquisition of Ultrasound and Gamma Signals with a Single-Channel Readout. Sensors. 2021;21(4):1048.

144. Yang Y, Biswal NC, Wang T, Kumavor PD, Karimeddini M, Vento J, et al. Potential role of a hybrid intraoperative probe based on OCT and positron detection for ovarian cancer detection and characterization. Biomed Opt Express. 2011;2(7):1918–30.

145. Povoski SP, Neff RL, Mojzisik CM, O'Malley DM, Hinkle GH, Hall NC, et al. A comprehensive overview of radioguided surgery using gamma detection probe technology. World J Surg Oncol. 2009;7(1):11.

146. Vidal-Sicart S, Seva A, Campos F, Sánchez N, Alonso I, Pahisa J, et al. Clinical use of an opto-nuclear probe for hybrid sentinel node biopsy guidance: first results. Int J Comput Assist Radiol Surg. 2019;14(2):409–16.

147. Winter A, Woenkhaus J, Wawroschek F. A Novel Method for Intraoperative Sentinel Lymph Node Detection in Prostate Cancer Patients Using Superparamagnetic Iron Oxide Nanoparticles and a Handheld Magnetometer: The Initial Clinical Experience. Ann Surg Oncol. 2014;21(13):4390–6.

148. DSouza A, Lin H, Henderson E, Samkoe K, Pogue B. Review of fluorescence guided surgery systems: identification of key performance capabilities beyond indocyanine green imaging. Journal of Biomedical Optics. 2016;21(8):080901.

149. Tsuchimochi M, Hayama K. Intraoperative gamma cameras for radioguided surgery: Technical characteristics, performance parameters, and clinical applications. Physica Med. 2013;29(2):126–38.

150. van Oosterom MN, Simon H, Mengus L, Welling MM, van der Poel HG, van den Berg NS, et al. Revolutionizing (robot-assisted) laparoscopic gamma tracing using a drop-in gamma probe technology. Am J Nucl Med Mol Imaging. 2016;6(1):1–17.

151. van Oosterom MN, Simon H, Mengus L, Welling MM, van der Poel HG, van den Berg NS, et al. Revolutionizing (robot-assisted) laparoscopic gamma tracing using a drop-in gamma probe technology. Am J Nucl Med Mol Imaging. 2016;6(1):1–17.

152. Matsui A, Tanaka E, Choi HS, Winer JH, Kianzad V, Gioux S, et al. Real-time intra-operative near-infrared fluorescence identification of the extrahepatic bile ducts using clinically available contrast agents. Surgery. 2010;148(1):87–95.

153. Alenezi A, Motiwala A, Eves S, Gray R, Thomas A, Meiers I, et al. Robotic assisted laparoscopic partial nephrectomy using contrast-enhanced ultrasound scan to map renal blood flow. Int J Med Robot. 2017;13(1).

154. Rao AR, Gray R, Mayer E, Motiwala H, Laniado M, Karim O. Occlusion angiography using intraoperative contrast-enhanced ultrasound scan (CEUS): a novel technique demonstrating segmental renal blood supply to assist zero-ischaemia robot-assisted partial nephrectomy. Eur Urol. 2013;63(5):913–9.

155. Dell'Oglio P, Meershoek P, Maurer T, Wit EMK, van Leeuwen PJ, van der Poel HG, et al. A DROP-IN Gamma Probe for Robot-assisted Radioguided Surgery of Lymph Nodes During Radical Prostatectomy. Eur Urol. 2021;79(1):124–32.

156. Collamati F, van Oosterom MN, De Simoni M, Faccini R, Fischetti M, Mancini Terracciano C, et al. A DROP-IN beta probe for robot-assisted 68Ga-PSMA radioguided surgery: first ex vivo technology evaluation using prostate specimens. EJNMMI Res. 2020;10(1):92.

157. van den Berg NS, Valdés-Olmos RA, van der Poel HG, van Leeuwen FWB. Sentinel Lymph Node Biopsy for Prostate Cancer: A Hybrid Approach. J Nucl Med. 2013;54(4):493–6.

158. Waelkens P, van Oosterom MN, van den Berg NS, Navab N, van Leeuwen FWB. Surgical Navigation: An Overview of the State-of-the-Art Clinical Applications. In: Herrmann K, Nieweg OE, Povoski SP, editors. Radioguided Surgery: Current Applications and Innovative Directions in Clinical Practice. Cham: Springer International Publishing; 2016. p. 57–73.

159. Kubicek J, Tomanec F, Cerny M, Vilimek D, Kalova M, Oczka D. Recent Trends, Technical Concepts and Components of Computer-Assisted Orthopedic Surgery Systems: A Comprehensive Review. Sensors. 2019;19(23):5199.

160. Citardi MJ, Yao W, Luong A. Next-Generation Surgical Navigation Systems in Sinus and Skull Base Surgery. Otolaryngol Clin North Am. 2017;50(3):617–32.

161. Chen X, Xu L, Wang Y, Hao Y, Wang L. Image-guided installation of 3D-printed patient-specific implant and its application in pelvic tumor resection and reconstruction surgery. Comput Methods Programs Biomed. 2016;125:66–78.

162. Calandri M, Mauri G, Yevich S, Gazzera C, Basile D, Gatti M, et al. Fusion Imaging and Virtual Navigation to Guide Percutaneous Thermal Ablation of Hepatocellular Carcinoma: A Review of the Literature. Cardiovasc Intervent Radiol. 2019;42(5):639–47.

163. Boekestijn I, Azargoshasb S, Schilling C, Navab N, Rietbergen D, van Oosterom MN. PET- and SPECT-based navigation strategies to advance procedural accuracy in interventional radiology and image-guided surgery. Q J Nucl Med Mol Imaging. 2021;65(3):244–60.

164. Bo X-W, Xu H-X, Wang D, Guo L-H, Sun L-P, Li X-L, et al. Fusion imaging of contrast-enhanced ultrasound and contrast-enhanced CT or MRI before radiofrequency ablation for liver cancers. Br J Radiol. 2016;89(1067):20160379.

165. Bluemel C, Safak G, Cramer A, Wöckel A, Gesierich A, Hartmann E, et al. Fusion of freehand SPECT and ultrasound: First experience in preoperative localization of sentinel lymph nodes. Eur J Nucl Med Mol Imaging. 2016;43(13):2304–12.

166. Bowles H, Sánchez N, Tapias A, Paredes P, Campos F, Bluemel C, et al. Radioguided surgery and the GOSTT concept: From pre-operative image and intraoperative navigation to image-assisted excision. Rev Esp Med Nucl Imagen Mol. 2017;36(3):175–84.

167. KleinJan GH, van den Berg NS, van Oosterom MN, Wendler T, Miwa M, Bex A, et al. Toward (Hybrid) Navigation of a Fluorescence Camera in an Open Surgery Setting. J Nucl Med. 2016;57(10):1650–3.

168. Oosterom MNv, Meershoek P, KleinJan GH, Hendricksen K, Navab N, Velde CJHvd, et al. Navigation of Fluorescence Cameras during Soft

Tissue Surgery—Is it Possible to Use a Single Navigation Setup for Various Open and Laparoscopic Urological Surgery Applications? Journal of Urology. 2018;199(4):1061–8.

169. Saß B, Bopp M, Nimsky C, Carl B. Navigated 3-Dimensional Intra-operative Ultrasound for Spine Surgery. World Neurosurgery. 2019;131:e155–69.

170. Wendler T, Traub J, Ziegler SI, Navab N, editors. Navigated Three Dimensional Beta Probe for Optimal Cancer Resection 2006; Berlin, Heidelberg: Springer Berlin Heidelberg.

171. Wendler T, Herrmann K, Schnelzer A, Lasser T, Traub J, Kutter O, et al. First demonstration of 3-D lymphatic mapping in breast cancer using freehand SPECT. Eur J Nucl Med Mol Imaging. 2010;37(8):1452–61.

172. Oosterom MNv, Meershoek P, Welling MM, Pinto F, Matthies P, Simon H, et al. Extending the Hybrid Surgical Guidance Concept With Freehand Fluorescence Tomography. IEEE Transactions on Medical Imaging. 2020;39(1):226–35.

173. Azargoshasb S, Molenaar L, Rosiello G, Buckle T, van Willigen DM, van de Loosdrecht MM, et al. Advancing intraoperative magnetic tracing using 3D freehand magnetic particle imaging. Int J Comput Assist Radiol Surg. 2022;17(1):211–8.

174. van Oosterom MN, Engelen MA, van den Berg NS, KleinJan GH, van der Poel HG, Wendler T, et al. Navigation of a robot-integrated fluorescence laparoscope in preoperative SPECT/CT and intraoperative freehand SPECT imaging data: a phantom study. J Biomed Opt. 2016;21(8):086008.

175. KleinJan GH, Karakullukçu B, Klop WMC, Engelen T, van den Berg NS, van Leeuwen FWB. Introducing navigation during melanoma-related sentinel lymph node procedures in the head-and-neck region. EJNMMI Res. 2017;7(1):65.

176. Fuerst B, Sprung J, Pinto F, Frisch B, Wendler T, Simon H, et al. First Robotic SPECT for Minimally Invasive Sentinel Lymph Node Mapping. IEEE Trans Med Imaging. 2016;35(3):830–4.

177. Kido S, Hirano Y, Mabu S. Deep Learning for Pulmonary Image Analysis: Classification, Detection, and Segmentation. In: Lee G, Fujita H, editors. Deep Learning in Medical Image Analysis : Challenges and Applications. Cham: Springer International Publishing; 2020. p. 47–58.

178. Laios A, Volpi D, Tullis IDC, Woodward M, Kennedy S, Pathiraja PNJ, et al. A prospective pilot study of detection of sentinel lymph nodes in gynaecological cancers using a novel near infrared fluorescence imaging system. BMC Res Notes. 2015;8(1):608.

179. Ladurner R, Lerchenberger M, Al Arabi N, Gallwas JKS, Stepp H, Hallfeldt KKJ. Parathyroid Autofluorescence—How Does It Affect Parathyroid and Thyroid Surgery? A 5 Year Experience. Molecules (Basel, Switzerland). 2019;24(14):2560.

180. Meershoek P, KleinJan GH, van Oosterom MN, Wit EM, van Willigen DM, Bauwens KP, et al. Multispectral fluorescence imaging as a tool to separate healthy and disease related lymphatic anatomies during robot-assisted laparoscopic procedures. J Nucl Med. 2018;59(11):1757–60.

181. de Vries HM, Bekers E, van Oosterom MN, Krakullukcu MB, van der Poel HG, van Leeuwen FWB, et al. c-MET receptor-targeted fluorescence on the road to image-guided surgery in penile squamous cell carcinoma patients. J Nucl Med. 2022;63(1):51–6.

182. Marsh JN, Matlock MK, Kudose S, Liu TC, Stappenbeck TS, Gaut JP, et al. Deep Learning Global Glomerulosclerosis in Transplant Kidney Frozen Sections. IEEE Trans Med Imaging. 2018;37(12):2718–28.

183. Azargoshasb S, van Alphen S, Slof LJ, Rosiello G, Puliatti S, van Leeuwen SI, et al. The Click-On gamma probe, a second-generation tethered robotic gamma probe that improves dexterity and surgical decision-making. Eur J Nucl Med Mol I. 2021;48(13):4142–51.

184. Wendler T, van Leeuwen FWB, Navab N, van Oosterom MN. How molecular imaging will enable robotic precision surgery. Eur J Nucl Med Mol I. 2021;48(13):4201–24.

185. Stummer W, Pichlmeier U, Meinel T, Wiestler OD, Zanella F, Reulen HJ. Fluorescence-guided surgery with 5-aminolevulinic acid for resection of malignant glioma: a randomised controlled multicentre phase III trial. Lancet Oncol. 2006;7(5):392–401.

186. Morton DL, Thompson JF, Cochran AJ, Mozzillo N, Nieweg OE, Roses DF, et al. Final Trial Report of Sentinel-Node Biopsy versus Nodal Observation in Melanoma. N Engl J Med. 2014;370(7):599–609.

187. Mazzone E, Dell'Oglio P, Grivas N, Wit E, Donswijk M, Briganti A, et al. Diagnostic Value, Oncologic Outcomes, and Safety Profile of Image-Guided Surgery Technologies During Robot-Assisted Lymph Node Dissection with Sentinel Node Biopsy for Prostate Cancer. J Nucl Med. 2021;62(10):1363–71.

188. KleinJan GH, van Werkhoven E, van den Berg NS, Karakullukcu MB, Zijlmans H, van der Hage JA, et al. The best of both worlds: a hybrid approach for optimal pre- and intraoperative identification of sentinel lymph nodes. Eur J Nucl Med Mol Imaging. 2018;45(11):1915–25.

189. Horn T, Krönke M, Rauscher I, Haller B, Robu S, Wester HJ, et al. Single Lesion on Prostate-specific Membrane Antigen-ligand Positron Emission Tomography and Low Prostate-specific Antigen Are Prognostic Factors for a Favorable Biochemical Response to Prostate-specific Membrane Antigen-targeted Radioguided Surgery in Recurrent Prostate Cancer. Eur Urol. 2019;76(4):517–23.

190. Knipper S, Mehdi Irai M, Simon R, Koehler D, Rauscher I, Eiber M, et al. Cohort Study of Oligorecurrent Prostate Cancer Patients: Oncological Outcomes of Patients Treated with Salvage Lymph Node Dissection via Prostate-specific Membrane Antigen-radioguided Surgery. Eur Urol. 2022;S0302–2838(22):02408–13.

191. Reiley CE, Lin HC, Yuh DD, Hager GD. Review of methods for objective surgical skill evaluation. Surg Endosc. 2011;25(2):356–66.

192. Estrada S, Malley MKO, Duran C, Schulz D, Bismuth J, editors. On the development of objective metrics for surgical skills evaluation based on tool motion. 2014 IEEE International Conference on Systems, Man, and Cybernetics (SMC); 2014 5–8 Oct. 2014.

193. Gordon I, Paoloni M, Mazcko C, Khanna C. The Comparative Oncology Trials Consortium: using spontaneously occurring cancers in dogs to inform the cancer drug development pathway. PLoS Med. 2009;6(10):e1000161.

194. Schlake A, Dell'Oglio P, Devriendt N, Stammeleer L, Binetti A, Bauwens K, et al. First robot-assisted radical prostatectomy in a client-owned Bernese mountain dog with prostatic adenocarcinoma. Vet Surg. 2020;49(7):1458–66.

195. van der Poel HG, Buckle T, Brouwer OR, Valdés Olmos RA, van Leeuwen FW. Intraoperative laparoscopic fluorescence guidance to the sentinel lymph node in prostate cancer patients: clinical proof of concept of an integrated functional imaging approach using a multimodal tracer. Eur Urol. 2011;60(4):826–33.

196. Schaafsma BE, Verbeek FPR, Rietbergen DDD, Hiel B, Vorst JR, Liefers GJ, et al. Clinical trial of combined radio- and fluorescence-guided sentinel lymph node biopsy in breast cancer. Br J Surg. 2013;100(8):1037–44.

197. Baiocchi GL, Guercioni G, Vettoretto N, Scabini S, Millo P, Muratore A, et al. ICG fluorescence imaging in colorectal surgery: a snapshot from the ICRAL study group. BMC Surg. 2021;21(1):190.

Publisher's Note